# Exact Matched Filter Performance Bound for Multitone Modulation in Fading Channels

Andrea M. Tonello
DIEGM - University of Udine
33100 Udine, Italy
tonello@diegm.uniud.it

**Abstract — We compute the exact matched filter performance bound for multitone modulated signals in time-variant frequency selective fading channels. The bound gives the probability of error that is achievable with ideal maximum likelihood detection. The computation is done following an exact calculation. This study allows for an analytical treatment of the diversity effect on performance as a function of the channel time and frequency selectivity. It is found that filtered multitone modulation is a diversity transform that is capable of yielding coding gains and time/frequency diversity gains as a function of the sub-carrier spacing, and the sub-channel filter shape.**

***Keywords* — *Diversity, fading channels, filtered multitone modulation, matched filter bound, OFDM, optimal detection.***

## 1. Introduction

In this paper we derive analytical expressions for the distribution and the average of the bit-error-rate for filtered multitone (FMT) modulation [1] over time-variant frequency selective fading channels when ideal maximum likelihood detection is deployed [5]-[8]. We already attacked the problem of determining the MFB performance in [6]. However, the study in [6] was based on the deployment of the Chernoff bounding technique, and it did not provide an exact analytical expression. Instead, in this paper, we study the exact MFB performance of FMT modulation. Analytical expressions for both the distribution and the average of the bit-error-rate are derived. These are obtained by first developing an equivalent discrete-time doubly dispersive channel model. Then, we derive the distribution of the squared distance that is associated to a pairwise error event. Such a distribution is obtained with the method of the residues, which is feasible once it is recognized that the squared distance can be written as a normal quadratic form [7].

With FMT modulation, a high rate information data symbol sequence is converted into a number of low rate sub-sequences. Each low rate sequence is transmitted over a sub-channel that is shaped with an appropriate filter centered on a given sub-carrier. When the sub-carriers are uniformly spaced and the sub-channel filters are identical, the efficient digital implementation is based on a FFT and low rate polyphase filtering. Discrete multitone modulation (DMT) is a particular implementation that deploys rectangular time domain filters such that the sub-channel filtering operation is avoided. DMT is also referred to as orthogonal frequency division multiplexing (OFDM). In general the frequency selectivity of the channel introduces intercarrier (ICI) and intersymbol (ISI) interference at the receiver side. The design of the sub-channel filters, and the choice of the sub-carrier spacing in an FMT system aims at subdividing the spectrum in a number of sub-channels that do not overlap in the frequency domain, such that we can avoid the ICI, and get low ISI contributions. In a DMT system the insertion of a cyclic prefix longer then the channel time dispersion is such that ISI and ICI are eliminated and the receiver simplifies to a simple one-tap equalizer per sub-channel. The channel temporal selectivity can also introduce ICI as a result of a loss of the sub-channels orthogonality. This happens when the channel is not static over the duration of the FFT block.

The presence of ISI and ICI is such that some form of multichannel equalization is required. We herein consider the deployment of optimal maximum-likelihood equalization [5]-[8]. For uncoded transmission, a limit on the best attainable performance is given by the probability of error achieved with perfect equalization, i.e., *matched filter performance bound* (MFB). That is, the bit-error-rate achieved when the equalizer is capable of canceling all interference components. The analysis of the matched filter performance bound has attracted considerable attention in various wireless communication scenarios (see, for instance, Clark *et al.* [2], Baas *et al.* [3]). These studies are interesting because they allow for an analytical treatment of the diversity effect on performance as a function of the channel time and frequency selectivity.

The analysis of the MFB performance reveals that FMT modulation can be interpreted as a diversity transform. When optimally detected, FMT modulation is capable of yielding coding and diversity gains as a function of the sub-channel filter impulse response, the number of tones, and the time-frequency characteristics of the channel. In general an increase in the number of sub-carriers translates into a loss of achievable frequency diversity gain, but into an increase in the time diversity gain. On the contrary, DMT modulation with cyclic prefix and conventional detection (OFDM) does not allow for any frequency diversity exploitation. Further, it suffers from the intercarrier interference introduced by time-variant fading such that a significant error floor is introduced.

A comprehensive set of numerical results is reported to substantiate such conclusions.

## 2. System Model

We consider a discrete-time implementation of a multicarrier modulator. The complex lowpass multitone modulated signal can be written as

$$x(iT) = \sum_{k\in\mathcal{K}} \sum_{l\in\mathbb{Z}} a^k(lT_0) g(iT - lT_0) e^{j2\pi f_k iT} \qquad i \in \mathbb{Z} \qquad (1)$$

where $a^k(lT_0)$ is the sequence of complex data symbols (e.g., M-QAM or M-PSK) transmitted on sub-channel $k$ at rate $1/T_0$

Part of this work was supported by MIUR under project FIRB "Reconfigurable platforms for wideband wireless communications", prot. RBNE018RFY.

with $T_0 = NT$ ; $g(t)$ is a sub-channel shaping filter (*prototype filter*); $\mathcal{K}$={0,…,*M*-1} is the set of sub-carrier indices *k*. The sub-channel carrier frequency is $f_k$, and in general $N \geq M$ . If we define the *sub-channel transmit filter* as $g_T^k(t) = g(t)e^{j2\pi f_k t}$ (frequency shifted prototype pulse), and $\tilde{a}^k(lT_0) = e^{j2\pi f_k lT_0} a^k(lT_0)$ we can write

$$x(iT) = \sum_{k\in\mathcal{K}} \sum_{l\in\mathbb{Z}} \tilde{a}^k(lT_0) g_T^k(iT - lT_0) \qquad i \in \mathbb{Z} \tag{2}$$

An efficient implementation, referred to as *filtered multitone modulation*, is possible when the sub-carriers are uniformly spaced, i.e., $f_k = k/T_1$ with $T_1 = MT$ . It comprises the S/P conversion of the data symbol stream, an M-point IFFT, and low-rate sub-channel (polyphase) filtering [1]. With minimal sub-carrier spacing (critically sampled FMT system) $N = M$ , and $\tilde{a}^k(lT_0) = a^k(lT_0)$ . The prototype pulse has nominal bandwidth $1/T_0 \leq 1/T_1$ that, for fixed *T*, becomes smaller as the number of sub-carriers increases. With a sufficiently high number of sub-carriers the unfolded spectrum of (1) has width almost entirely confined in 1/*T*, which can be practically achieved by avoiding transmission over some of the outermost sub-carriers. As an example, in this paper we consider the deployment of rectangular time domain prototype pulses, rectangular frequency domain pulses, and Gaussian pulses:

$$g_{\text{rect}}(i) = g_{\text{rect}}(iT) = \frac{1}{\sqrt{N}} \text{rect}(\frac{i}{N}) ,$$

$$g_{\text{sinc}}(i) = \frac{1}{\sqrt{N}} \text{sinc}(\frac{i}{N}) , \qquad g_{\text{gauss}}(i) = \sqrt{\frac{\sigma}{N}} \sqrt[4]{\frac{2}{\pi}} e^{-(\sigma i/N)^2} \tag{3}$$

where $\sigma = B\pi\sqrt{2/\ln 2}$ , and *B* normalized bandwidth. Note that the Gaussian pulses have the interesting property of having concentrated impulse and frequency response.

The MT signal (1) is digital-to-analog converted, RF modulated, and transmitted over the air. The received signal is RF demodulated, and analog-to-digital converted. The sequence of received samples at rate $1/T$ can be written as

$$y(iT) = \sum_{n\in\mathbb{Z}} x(nT) h_E(iT - nT; iT) + w(iT) \tag{4}$$

where $w(iT)$ is a sequence of i.i.d. circularly symmetric Gaussian random variables with zero-mean, and variance $N_0$ . $h_E(\tau;t)$ is the equivalent impulse response that comprises the DAC/ADC filters, and the frequency selective time-variant fading channel. We assume the channel to be practically time-invariant over the duration of the ADC filter whose main lobe has duration ~2*T*. However, we emphasize that the channel is not necessarily static over the duration of the prototype pulse. Conventionally, the analog filters in the DAC and ADC are square-root raised cosine filters.

If we define the equivalent sub-channel receive filter as $g_R^k(\tau;t) = \sum_{i\in\mathbb{Z}} g_T^k(iT) h_E(\tau - iT; t)$ the broadband received signal can be written as the sum of *M* narrowband signals:

$$y(iT) = \sum_{k\in\mathcal{K}} \sum_{l\in\mathbb{Z}} \tilde{a}^k(lT_0) g_R^k(iT - lT_0; iT) + w(iT) . \tag{5}$$

We can represent the discrete-time equivalent channel impulse response with a T-spaced tapped delay line

$$h_E(nT; iT) = \sum_{p\in\mathcal{P}} \alpha_p(iT) \delta(nT - pT) \qquad \mathcal{P} = \{-N_P, ..., N_P\} \tag{6}$$

that has Gaussian distributed tap gains with a certain correlation. We assume wide sense stationary uncorrelated scattering (WSSUS), and a common time selective correlation function across the delay profile [3], [7]. Let $\phi_g(t)$ denote the delay power spectrum, $\psi_d(t)$ the time-selective correlation function, and $g_B(t)$ the ADC+DAC impulse response. Then, the equivalent channel autocorrelation reads

$$E[h_E(\tau_1;t_1) h_E^*(\tau_2;t_2)] = \psi_d(t_2 - t_1) \int_{\mathbb{R}} \phi_g(\tau_3) g_B(\tau_1 - \tau_3) g_B^*(\tau_2 - \tau_3) d\tau_3 \tag{7}$$

The analysis the follows is sufficiently general, and the results apply to general delay power spectrum, and Doppler spectrum models. However, for the delay power spectrum we mostly focus on the one sided exponential [2] or the 3GPP-ITU models [10]. For the Doppler spectrum we use the Jakes' model that is derived under the assumption of isotropic scattering. For this model $\psi_d(t) = J_0(2\pi f_d t)$ where $J_0(t)$ denotes the zero-order Bessel function of the first kind, and $f_d$ is the one-sided Doppler spread.

Throughout this paper we use matrix notation. In particular, we denote the channel taps mean vector with $\mathbf{m} = E[\boldsymbol{\alpha}]$ , and the correlation matrix with $\mathbf{R} = E[\boldsymbol{\alpha}\boldsymbol{\alpha}^H]$ where the vector $\boldsymbol{\alpha}$ is defined as

$$\boldsymbol{\alpha} = [\boldsymbol{\alpha}_{-L}^T, ..., \boldsymbol{\alpha}_L^T]^T \qquad \boldsymbol{\alpha}_i = [\alpha_{-N_P}(iT), ..., \alpha_{N_P}(iT)]^T \tag{8}$$

for given integers $N_P$ , and $L$ . The correlation matrix is Hermitian, with size $(2N_P + 1)(2L + 1)$ . If we use numerical integration of (7), we can now write [7]

$$\mathbf{R} = E[\boldsymbol{\alpha}\boldsymbol{\alpha}^H] = toeplitz\{\mathbf{G}_B^H \boldsymbol{\Phi}_0 \mathbf{G}_B, ..., \mathbf{G}_B^H \boldsymbol{\Phi}_{2L} \mathbf{G}_B\} \tag{9}$$

$$\boldsymbol{\Phi}_i = J_0(2\pi f_d iT) diag\{\phi_{-N_L}, ..., \phi_{N_L}\} \tag{10}$$

$$\mathbf{G}_B = \begin{bmatrix} g_B(-N_P T + N_L T_c) & ... & g_B(N_P T + N_L T_c) \\ ... & ... & ... \\ g_B(-N_P T - N_L T_c) & ... & g_B(N_P T - N_L T_c) \end{bmatrix} \tag{11}$$

with $\phi_l = T_c \phi_g(lT_c)$ , $T_c = T/K$ , and $K \geq 1$ .

## 3. Optimal Multitone Detection

Details about the optimal multitone detector can be found in [6], [7], and in [5], [8] for the more general multiuser scenario. It basically consists of a bi-dimensional equalizer that deals with both the ICI and the ISI implementing a Viterbi algorithm with an appropriate metric. Under certain conditions it simplifies into a bank of single channel Viterbi equalizers. Given the model in (5), the optimal maximum likelihood detector seeks the data sequence $\mathbf{b} = \{b^k(lT_0)\}$ , $k \in \mathcal{K}$ , $l \in \mathbb{Z}$ , that minimizes the Euclidean distance $\Delta = \sum_{i\in\mathbb{Z}} | y(iT) - -\sum_{l\in\mathbb{Z}} \sum_{k\in\mathcal{K}} \tilde{b}^k(lT_0) g_R^k(iT - lT_0; iT) |^2$ . If the channel is static, the sub-channel filters are band limited, and they do not overlap in the frequency domain, the multichannel detector simplifies to *M* single channel equalizers [7]. With *sinc* pulses (ideal FMT) such conditions are met. With *rect* pulses (DMT) the presence of intercarrier interference requires to jointly detect all sub-channels. In the latter case simplified detection is possible when deploying a cyclic prefix, which is usually referred to as OFDM with cyclic prefix. If the prototype filter is time limited, e.g, with DMT modulation, a time-variant channel does not introduce ISI. However, ICI is present such that the optimal

detector still requires to jointly detect all sub-channels [7]. From a complexity standpoint the deployment of practically time and frequency concentrated pulses should be pursued. On the contrary from a performance standpoint this conclusion is not necessarily true, as we will show in the next section.

## 4. Exact Matched Filter Bound Performance

Under the hypothesis of perfect knowledge of the channel state information $\mathbf{s}$, the *pairwise error probability* (PEP), i.e., the probability that the optimal MT detector decides erroneously in favor of the sequence $\mathbf{b}=\{b^k(lT_0)\}$, $k\in\mathcal{K}$, $l\in\mathbb{Z}$, when $\mathbf{a}=\{a^k(lT_0)\}$ was indeed transmitted, is given by $P(\mathbf{a}\to\mathbf{b}\,|\,\mathbf{s})=Q\left(\sqrt{d^2(\mathbf{a},\mathbf{b})/(2N_0)}\right)$ where the *pairwise error event distance* reads (12)

$$d^2(\mathbf{a},\mathbf{b})=\sum_{i\in\mathbb{Z}}\Big|\sum_{l\in\mathbb{Z}}\sum_{k\in\mathcal{K}}\underbrace{e^{j2\pi f_k lT_0}[a^k(lT_0)-b^k(lT_0)]}_{e^k(lT_0)}g_R^k(iT-lT_0;iT)\Big|^2 .$$

If we consider uncoded transmission, single error events are possible, i.e., the detected sequence may differ only in one data symbol from the transmitted sequence. The evaluation of such pairwise error probability yields a lower bound (performance limit) on the symbol error probability. In fact, this is the error probability achieved with perfect equalization. In literature it is referred to as matched filter performance bound (MFB) [2], [3]. Let us assume the single error event to occur on sub-channel $k$, and time instant $lT_0$. Then, the error event distance can be written as follows

$$\begin{aligned}d^2_{MFB}(k,l)=D_e s^{k,k}(l,l)=D_e\sum_{i\in\mathbb{Z}}\sum_{p,\,p'\in\mathcal{P}}\alpha_p^*(iT+lT_0)\alpha_{p'}(iT+lT_0)\\ \times e^{j2\pi f_k(pT-p'T)}g^*(iT-pT)g(iT-p'T)\end{aligned} \quad (13)$$

where $D_e=|\,e^k(lT_0)\,|^2$ is the squared Euclidean distance between the transmitted, and the detected data symbol, e.g., with BPSK signaling $D_e=4E_S$.

In general (13) is a function of the sub-channel index, and the time instant. To proceed, let us assume the channel response, and the prototype pulse to have (practically) finite duration. Then, $\mathcal{P}=\{-N_P,...,N_P\}$, and $g(iT)=0$ for $i\notin\{-N_g,...,N_g\}$. Setting $L=N_g+N_P$, with matrix notation we obtain

$$d^2_{MFB}(k,l)=D_e\sum_{i\in\mathbb{Z}}\boldsymbol{\alpha}^H_{i+lN}\mathbf{W}^H_{k,0}\mathbf{G}_i\mathbf{W}_{k,0}\boldsymbol{\alpha}_{i+lN}=\boldsymbol{\alpha}^H\mathbf{W}_k^H\mathbf{G}\mathbf{W}_k\boldsymbol{\alpha} \quad (14)$$

where $\mathbf{g}_i=[g(iT+N_PT),...,g(iT-N_PT)]^T$, $\mathbf{G}_i=\mathbf{g}_i^*\mathbf{g}_i^T$, $\mathbf{G}=diag\{\mathbf{G}_{-L},...,\mathbf{G}_L\}$, $\mathbf{W}_{k,0}=diag\{e^{-j2\pi f_k N_PT},...,e^{j2\pi f_k N_PT}\}$, and $\mathbf{W}_k=diag\{\underbrace{\mathbf{W}_{k,0},...,\mathbf{W}_{k,0}}_{2L+1}\}$. Since the vector of channel taps $\boldsymbol{\alpha}$ is Gaussian, (14) is a normal quadratic form (see [7] for details).

We emphasize that when the channel impulse response is sparse, it is possible to reduce the size of the vectors and matrices in (14) by deleting the zero components of $\boldsymbol{\alpha}$ and the corresponding rows and columns in $\mathbf{G}$ and $\mathbf{W}_k$. Assuming $\mathbf{R}$ to be full rank, and the channel taps to have zero mean (Rayleigh fading), the squared MFB distance can be rewritten as [4], [7]

$$d^2_{MFB}(k)=\sum_{i=1}^{N_\lambda}\lambda_i\,|\,\beta_i\,|^2 \quad (15)$$

where $\lambda_i$ are the $N_\lambda$ eigenvalues of the matrix $D_e\mathbf{R}\mathbf{W}_k^H\mathbf{G}\mathbf{W}_k=D_e\mathbf{R}\mathbf{G}_k$, and $\beta_i$ are i.i.d. complex Gaussian random variables with zero mean, and unit variance. Note that we have dropped the dependency on $l$ since we are in stationary conditions. The probability density function, $p_{d^2_{MFB}}(a)$, and the probability distribution function, $F_{d^2_{MFB}}(a)$, of (15) can be found through the inversion of the characteristic function (see [2], and [7]). Let us assume to have $N'$ out of $N_\lambda$ distinct eigenvalues $\lambda_1,...,\lambda_{N'}$, each with multiplicity $m_1,...,m_{N'}$, then

$$p_{d^2_{MFB}}(a)=\sum_{i=1}^{N'}\sum_{n=1}^{m_i}A_{i,n}\frac{a^{n-1}}{\lambda_i^n(n-1)!}e^{-\frac{a}{\lambda_i}}1(a) \quad (16)$$

$$F_{d^2_{MFB}}(a)=\sum_{i=1}^{N'}\sum_{n=1}^{m_i}A_{i,n}\left(1-e^{-\frac{a}{\lambda_i}}\sum_{l=0}^{n-1}\left(\frac{a}{\lambda_i}\right)^l\frac{1}{l!}\right)1(a) \quad (17)$$

where $A_{i,n}$ are the coefficients of the partial fractions expansion of the characteristic function (residues)[1]

$$A_{i,n}=\frac{1}{(-\lambda_i)^{m_i-n}(m_i-n)!}\left[\frac{d^{m_i-n}}{ds^{m_i-n}}\left\{\prod_{p=1,\,p\neq i}^{N'}\left(1-\lambda_p s\right)^{-m_p}\right\}\right]_{s=1/\lambda_i} . \quad (18)$$

It follows that the distribution of the squared distance is a weighted sum of Erlang distributions.

Now, the average matched filter probability of error bound is computed as $P_{e,MFB}=\int_{R^+}Q(\sqrt{a/(2N_0)})p_{d^2_{MFB}}(a)da$. The integral can be evaluated in closed form (e.g., see [2]) yielding

$$P_{e,MFB}(k)=\frac{1}{2}\sum_{i=1}^{N'}\sum_{n=1}^{m_i}A_{i,n}\left[1-\sum_{l=0}^{n-1}\frac{(2l)!}{2^{2l}(l!)^2}\sqrt{\frac{\lambda_i/4N_0}{(1+\lambda_i/4N_0)^{2l+1}}}\right] . \quad (19)$$

For BPSK, and QPSK signaling the bit-error-rate on sub-carrier $k$, $BER(k)$, is given by (19) when $D_e$ is respectively set to $D_e=4E_S$, and $D_e=2E_S$. Further, the bit error-rate complementary distribution equals (17),

$$P[BER(k)\geq Q(\sqrt{a_0/2N_0})]=F_{d^2_{MFB}}(a_0) . \quad (20)$$

The average (across sub-channels) bit-error-rate can be defined as follows

$$BER=\sum_{k\in\mathcal{K}}BER(k)/M . \quad (21)$$

The analysis is sufficiently general to be applied to higher order constellations, e.g., M-QAM. We report numerical results corresponding to (19), (20), and (21) for various transmission scenarios in Section 6.

### 4.1 Gaussian Tail Function Bound

Using the Chernoff bound we can write that $P_{e,MFB}(k)\leq 0.5\exp(-1/4N_0\sum_{i=1}^{N_\lambda}\lambda_i\,|\,\beta_i\,|^2)$. Then, averaging over the distributions of $|\,\beta_i\,|^2$ (exponential) we obtain

$$P_{e,MFB}(k)\leq\frac{1}{2}\prod_{i=1}^{N_\lambda}\left(1+\frac{\lambda_i}{4N_0}\right)^{-1}\leq\frac{1}{2}\left(\frac{E_S}{4N_0}\right)^{-d}\prod_{\lambda_i\neq 0}\left(\frac{\lambda_i}{E_S}\right)^{-1} \quad (22)$$

where $d$ equals the number of nonzero eigenvalues. This upper bound is useful to understand how the sub-channel filter, and the sub-carrier spacing impact performance [6]. It reveals that

[1] With a single eigenvalue of multiplicity $m$, $A_{1,m}=1$ and $A_{1,j}=0$ for $j$=1,…,$m$-1. With $N$ distinct eigenvalues, $A_{1,1}=\prod_{p=1,\,p\neq i}^{N}1/\left(1-\lambda_p/\lambda_i\right)$. The step function is denoted with $1(a)$.

FMT modulation can be interpreted as a diversity transform that performs sub-channel time or spectrum spreading as a function of the prototype filter and the sub-carrier spacing, and in particular:

- FMT modulation with optimal detection provides both a *diversity gain*, and a *coding gain* over uncoded single carrier transmission through a flat Rayleigh fading channel. The diversity gain *d* equals the number of nonzero eigenvalues of $D_e\mathbf{RG}_k$, while the product of the nonzero eigenvalues gives the coding gain.
- The diversity gain satisfies the bound $d \le \min\{rank(\mathbf{R}), rank(\mathbf{G}_k)\}$. If the channel is frequency selective but time-invariant, then $1 \le d \le \widehat{N}_P$ with $\widehat{N}_P$ equal to the number of non-zero T-spaced channel taps. If the channel is frequency non-selective but time-variant, then $1 \le d \le \hat{L}$ with $\hat{L}T$ equal to the prototype pulse duration.

A detailed discussion is made in the next section, however, it is already clear that a sub-channel bandwidth expansion potentially increases the frequency diversity gain, while a sub-channel bandwidth compression (pulse duration expansion) increases the time diversity gain.

## 5. Analysis of the Results

In this section we dig into the probability of error assuming first a time-invariant frequency selective channel, and then a time-variant flat fading channel. These are two major scenarios that can be considered representative respectively of wide band communications and narrow band communications.

### 5.1 Time-Invariant Frequency Selective Channel

If the channel is time-invariant frequency selective we can re-write the squared error distance as follows

$$d^2_{MFB}(k) = D_e \boldsymbol{\alpha}_0^H \mathbf{W}_{k,0}^H \boldsymbol{\kappa} \mathbf{W}_{k,0} \boldsymbol{\alpha}_0 = \sum_{i=1}^{2N_p+1} \lambda_i \mid \beta_i \mid^2 \qquad (23)$$

with $\boldsymbol{\kappa} = \sum_i \mathbf{G}_i$ being the prototype pulse autocorrelation matrix with elements $(\boldsymbol{\kappa})_{p,p'} = \sum_i g^*(iT) g(iT + pT - p'T)$. When we deploy a *rect* prototype pulse, a *sinc* prototype pulse, or a Gaussian prototype pulse the autocorrelation coefficients can be calculated in closed form (see [7]).

The eigenvalues in (23) are the ones associated to the matrix $D_e \mathbf{G}_B^H \boldsymbol{\Phi}_0 \mathbf{G}_B \mathbf{W}_k^H \boldsymbol{\kappa} \mathbf{W}_k$. When $\mathbf{G}_B^H \boldsymbol{\Phi}_0 \mathbf{G}_B$ is diagonal, i.e., when the T-spaced channel taps are uncorrelated, they are independent of the sub-carrier index *k*. Since we consider uncorrelated scattering, correlation among the T-spaced channel taps can be introduced by the filters in the DAC-ADC. If this is the case, the matched filter error rate bound may differ across sub-channels.

The results that we have obtained still hold with single carrier modulation. In such a case,

$$d^2_{MFB,M=N=1}(k) = D_e \boldsymbol{\alpha}_0^H \mathbf{I} \boldsymbol{\alpha}_0 = D_e \sum_{p \in \mathcal{P}} \mid \alpha_p \mid^2 \qquad (24)$$

and the eigenvalues to be determined are those of the matrix $D_e \mathbf{G}_B^H \boldsymbol{\Phi}_0 \mathbf{G}_B$. The matched filter performance bound takes into account the shape of the pulse in the DAC-ADC as well as the correlation among T-spaced channel taps. When the number of sub-carriers goes to infinity, the squared distance reads

$$d^2_{MFB,M=N\to\infty}(k) = D_e \boldsymbol{\alpha}_0^H \mathbf{F}_k \boldsymbol{\alpha}_0 \qquad (25)$$

where $\mathbf{F}_k = toepz\{[1,\ e^{-j2\pi f_k T},\ e^{-j2\pi f_k 2T},...,\ e^{-j2\pi f_k 2N_P T}]\}$. It has rank 1 therefore the matrix $\mathbf{RF}_k$ has also rank one with the only nonzero eigenvalue equal to $\lambda(k) = trace(\mathbf{RF}_k) = = \sum_n \sum_m R_{n,m} e^{j2\pi f_k (m-n)T}$. With uncorrelated taps the MFB goes to the error-rate that is achieved in flat fading since in such a case for all sub-channels $\bar{\lambda} = trace(\mathbf{RF}_k) = trace(\mathbf{R}) = 1$ with a normalized power delay profile. Note that with correlated taps, and a number of sub-carriers that goes to infinity, the average error-rate is not lower than that in flat fading (see [7]).

The above results tell us that with multicarrier transmission through a given frequency selective channel we get diminished frequency diversity gains as the number of sub-carriers increases, independently of the prototype pulse. However, an increase in the number of sub-carriers translates into a decrease of the detection complexity since the sub-channels tends to a have a flat frequency response. Clearly, for a given number of sub-carriers different pulses yield different performance.

### 5.2 Time-Variant Frequency Non-Selective Channel

If we assume the channel to be frequency nonselective (flat) but time-variant, we obtain

$$d^2_{MFB} = D_e \sum_{i\in\mathbb{Z}} \mid \alpha(iT) \mid^2 \mid g(iT) \mid^2 = D_e \hat{\boldsymbol{\alpha}}^H \hat{\mathbf{G}} \hat{\boldsymbol{\alpha}} = \sum_{i=1}^{2N_g+1} \lambda_i \mid \beta_i \mid^2 \qquad (26)$$

with $\hat{\boldsymbol{\alpha}} = [\alpha(-N_g T),...,\alpha(N_g T)]$, $\hat{\mathbf{G}} = diag\{\mid g(-N_g T)\mid^2,...,\mid g(N_g T)\mid^2\}$ and $\lambda_i$ are the eigenvalues of $D_e E[\hat{\boldsymbol{\alpha}}\hat{\boldsymbol{\alpha}}^H]\hat{\mathbf{G}} = D_e \hat{\mathbf{R}} \hat{\mathbf{G}}$. The squared distance is identical over all sub-channels.

If the channel is fully uncorrelated (ergodic) we have $2N_g + 1$ eigenvalues $\lambda_i = D_e \mid g(iT) \mid^2$. In particular with a *rect* prototype pulse we get one eigenvalue $\lambda_i = D_e / N$ with multiplicity $N$. It follows that an increase in the number of sub-carriers translates into increased temporal diversity gains. If the number of sub-carriers goes to infinity the distribution (17) goes to $F_{d^2}(a) = 1(a - D_e)$, i.e., the squared distance becomes deterministic (see [7]). Thus, the probability of error tends to the probability of error in the absence of fading (AWGN only).

With single carrier transmission we can write $d^2_{MFB,M=N=1} = D_e \mid \alpha(0) \mid^2$ therefore there is only one eigenvalue $\lambda = D_e$, and consequently there is no temporal diversity exploitation. Recall that we have assumed the channel to be static over the duration of the ADC filter.

### 5.3 DMT with Cyclic Prefix and Conventional Detection

In DMT-CP (OFDM with cyclic prefix) [9] if the channel is static over the duration of the prototype pulse and the guard time is longer than the channel dispersion, no ICI and no ISI are present, and the detector simplifies to a one-tap equalizer. If the channel is time variant, ICI is introduced. The point here is that although conventional detection of DMT-CP is simple, it does not exploit the frequency diversity, and it suffers from the ICI introduced by a fast time-variant channel (see [7] for details).

## 6. Numerical Examples

In this section we report several numerical results for the average, and the distribution of the bit-error-rate in various propagation conditions. A more comprehensive set of results can be found in [7]. We assume BPSK signaling, and square-root-raised cosine filters in the DAC, and ADC, with a roll-off factor equal to 0.22. We choose the prototype pulse to be either rectangular in time (*rect pulse*), or rectangular in frequency (*sinc pulse*), or Gaussian (*Gauss pulse*). The sub-carrier spacing

is minimal, i.e., $M=N$, $T_1=T_0$.

In Fig. 1 we show the MFB bit-error-rate distribution as a function of the sub-carrier index assuming $E_S/N_0$=11dB and a Guassian prototype pulse with normalized bandwidth $B = 0.33$. In the top figures the channel is assumed to experience quasi-static (time-invariant over the prototype pulse duration) Rayleigh fading with a one-sided exponential power delay profile with *rms* delay spread $\tau_0 = 6.5T$. As it can be seen in the top plots of Fig. 1 there is some variability in the bit-error rate distribution across the sub-channels. The outermost channels exhibit worse BER distribution. Further, as the number of sub-carriers increases from 9 to 129 the frequency diversity gain diminishes, as a result of a sub-channel bandwidth compression.

In the bottom plots of Fig. 1 we assume time-variant flat fading with a Jakes' Doppler spectrum having normalized Doppler $f_dT = 0.009$. The plots show that the bit-error-rate distribution is the same across the sub-channels. Now, as the number of sub-carriers increases the distribution of the bit-error-rate improves as the consequence of increased time-diversity exploitation.

In Fig. 2 we show the average BER for a frequency selective channel with the ITU Pedestrian B profile [10]. Solid curves report the exact MFB while the dashed curves correspond to the Chernoff upper bound. The bandwidth is $W$=3.84 MHz. OFDM with cyclic prefix and conventional detection performs the worst. The MFB BER performance is the best for the *rect* pulse. As the number of sub-carriers increases the performance worsens for all the pulses that are considered. Note that asymptotically the Chernoff bound curves have the correct slope and thus they give the correct diversity gain.

In Fig. 3 we show the average BER for a fast flat Rayleigh fading channel with a bandwidth of $W$=24.3 kHz. OFDM with conventional detection exhibits a high error floor. The MFB BER performance is the best for the *gauss* pulse, and it improves as the number of sub-carriers increases.

## 7. Conclusions

We have computed the exact matched filter bound performance of FMT modulation. It shows that with ideal equalization both a diversity and a coding gain are obtainable in time-variant frequency selective fading. The Chernoff bound computed in [6] gives, indeed, the correct diversity gain.

## References


[1] G. Cherubini, E. Eleftheriou, S. Olcer, J. Cioffi, "Filter bank modulation techniques for very high-speed digital subscriber lines", *IEEE Commun. Magazine*, pp. 98-104, May 2000.

[2] M. Clark, L. Greenstein, K. Kennedy, "Matched filter performance bounds for diversity combining receivers in digital mobile radio", IEEE Trans. on Vehicular Tech., vol. 41, no. 4, pp. 356-362, November 1992.

[3] N. Baas, D. Taylor, "Matched filter bounds for wireless communication over Rayleigh fading dispersive channels", *IEEE Trans. on Commun.*, vol. 49, pp. 1525-1528, September 2001.

[4] C. Schlegel, "Error probability calculation for multibeam Rayleigh channels", *IEEE Trans. on Comm.*, pp. 290-293, March 1996.

[5] A. Tonello, "Asynchronous multicarrier multiple access: optimal and sub-optimal detection and decoding", *Bell Labs Technical Journal vol. 7 n. 3*, pp. 191-217, February 2003.

[6] A. Tonello, "Performance limits of multicarrier based systems over fading channels with optimal detection", *Proc. of IEEE WPMC 02*, Honolulu, pp. 1005-1009, October 2002.

[7] A. Tonello, "Performance limits for filtered multitone modulation in fading channels", *subm. to IEEE Trans. Wireless Comm.*, April 2003.

[8] A. Tonello, "Multiuser detection and turbo multiuser decoding in asynchronous multitone multiple access systems", *IEEE WPMC 02*, Honolulu, October 2002.

[9] Z. Wang, G. Giannakis, "Wireless multicarrier communications", *IEEE Signal Processing Magazine*, pp. 29-48, May 2000.

[10] "Universal Mobile Telecommunication System (UMTS); Selection procedures for the choice of radio transmission technologies for the UMTS", TR 101.112, ETSI, 1998.


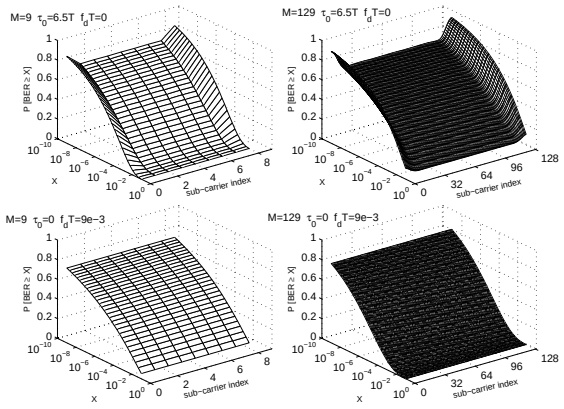


Fig. 1. BER distribution as a function of the sub-carrier index with $E_S/N_0$=11 dB and *Gaussian* sub-channel pulse. Frequency selective Rayleigh fading channel with exponential power delay profile (top plots). Flat Rayleigh fading channel with Jakes' Doppler spectrum (bottom plots).

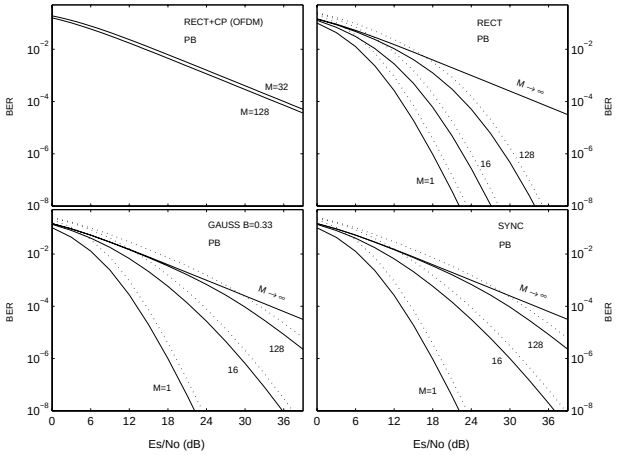


Fig.2. Average BER in ITU PB channel with quasi static fading and bandwidth W=3.84 MHz. Solid curves: exact value. Dashed curves: Chernoff upper bound.

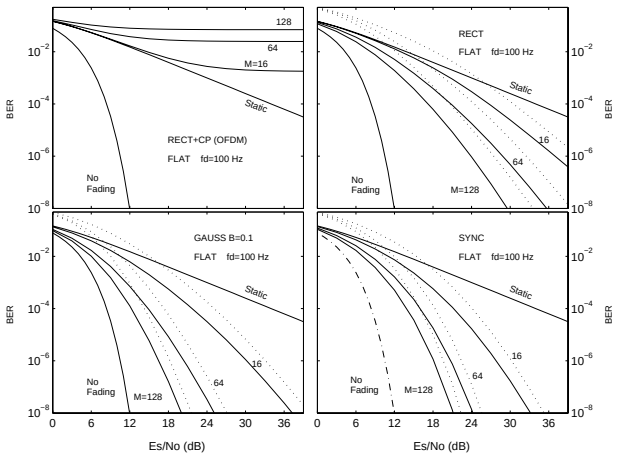


Fig.3. Average BER in flat fading with Jakes' Doppler spectrum and W=24.3 kHz. Solid curves: exact value. Dashed curves: Chernoff upper bound.